


# A Beam Projection-Based Modified Gamma Analysis Scheme for Clinically Interpretable Pre-Treatment Dose Verification

Dose-Response:  
An International Journal  
April-June 2021:1-7  
© The Author(s) 2021  
Article reuse guidelines:  
sagepub.com/journals-permissions  
DOI: 10.1177/15593258211001676  
journals.sagepub.com/home/dos



Yiling Wang<sup>1</sup> , Gang Yin<sup>1,2</sup>, Jie Wang<sup>1</sup>, Yue Zhao<sup>1</sup>, Min Liu<sup>1</sup>, and Jinyi Lang<sup>1</sup>

## Abstract

**Purpose:** To investigate a novel gamma analysis system for dose verification results in terms of clinical significance.

**Methods and Materials:** The modified scheme redefined the computational domain of the conventional gamma analysis with the projections of beams and the regions of interest (ROI). We retrospectively studied 6 patients with the conventional and the modified gamma analysis schemes while compared their performances. The cold spots ratio of the planning target volume (PTV) and the hot spots ratio of the organs at risk (OAR) were also computed by the modified scheme to assess the clinical significance.

**Results:** The result of the gamma passing rate in the modified method was conformable to that in the conventional method with a cut-off threshold of 5%. The cold spots ratio of PTV and hot spots ratio of OAR were able to be evaluated by the modified scheme. For an introduced 7.1% dose error, the discrimination ratio in gamma passing rate of the conventional method was lower than 2%, while it was improved to 5% by the modified method.

**Conclusions:** The modified gamma analysis scheme had a comparable quality as the conventional scheme in terms of dose inspection. Besides, it could improve the clinical significance of the QA result and provide the assessment for ROI-specific discrepancy. The modified scheme could also be conveniently integrated into the conventional dose verification process, benefiting the less developed regions where high-end 3D dose verification devices are not affordable.

## Keywords

pretreatment dose verification, gamma analysis, beam projection

## Introduction

Intensity-modulated radiation therapy (IMRT)<sup>1</sup> is widely utilized in the clinic, yielding complex dose distributions with sharp gradients.<sup>2</sup> To inspect whether the dose delivered by the linear accelerator is conformed with that in the treatment planning system (TPS), the pre-treatment quality assurance (QA) is routinely performed.<sup>3</sup> For instance, the gamma analysis is a standard approach for evaluating the fidelity of IMRT delivery with both the dose difference and the distance to agreement (DTA)<sup>4</sup> considered for the gamma passing rate (%GP). For the gamma analysis, the patient-specific plan is transplanted into a phantom commonly in a simple shape. Subsequently, the planned dose is recomputed and compared with the measured one by planar or cylindrical detector arrays.<sup>5,6</sup> If the dose discrepancy is acceptable for phantom, it is believed the dose discrepancy of clinical treatment can still maintain at that level. To conduct the gamma analysis, commercially available devices are MatriXX (IBA Dosimetry GmbH, Germany),<sup>5</sup>

ArcCHECK (SunNuclear Corporation, FL, USA),<sup>6</sup> and Delta (ScandiDos, Uppsala, Sweden),<sup>7</sup> etc.

Although the conventional planar gamma analysis is efficient and widely applicable for IMRT QA, there still leaves space for improvement indicated by several reports.<sup>1,8-10</sup> For

<sup>1</sup> Sichuan Cancer Hospital & Institute, School of Medicine, University of Electronic Science and Technology of China, Radiation Oncology Key Laboratory of Sichuan Province, Chengdu, China

<sup>2</sup> The First People's Hospital of Liangshan, Liangshan Yi Autonomous Prefecture, Sichuan, China

Received 13 December 2020; received revised 13 December 2020; accepted 18 February 2021

## Corresponding Author:

Gang Yin, Sichuan Cancer Hospital & Institute, School of Medicine, University of Electronic Science and Technology of China, Radiation Oncology Key Laboratory of Sichuan Province, Chengdu, China.

Email: cxqyguestc@163.com



instance, the traditional method can hardly interpret the discovered dose discrepancy in the sense of clinical significance, since the information of patient geometry was absent in the analysis. Furthermore, a rejected result can hardly render any insight into the clinical source of failure, resulting in difficulty in modifying the IMRT.

To evaluate the individualized dose discrepancy, several specially designed 3D systems could be applied, such as the Compass system (IBA Dosimetry GmbH, Germany),<sup>11</sup> and the 3DVH system (Sun Nuclear Corporation, FL, USA),<sup>12</sup> etc. However, they may introduce additional error during the 2D-to-3D dose transformation process, regarding that the deformable transformation process could be error-uncontrollable. It has been reported that the 3D QA results could be more variable and sensitive to errors in comparison with their 2D counterpart.<sup>10,12</sup> Besides, according to the literature,<sup>10</sup> the cumulative error could even be magnified during the 2D-to-3D transformation. Besides, with an additional 2D-to-3D computation, those 3D systems could also be less computationally efficient. Moreover, it could pose a burden on medical institutes, especially for those in less-developed regions, due to the investment for high-end verification devices.

The purpose of this study is to provide and investigate an in-house modified gamma analysis system to improve the clinical significance of the planar QA results. The projections of beams and regions of interest (ROI) are innovatively applied to redefine the computational domain of gamma analysis. The cold spots ratio of the planning target volume (PTV) and the hot spots ratio of the organs at risk (OAR) are planned for assessment. To our best knowledge, this is the first study that explores the potential of projections for the interpretation of 2D QA results in a sense of clinical significance.

## Materials and Methods

### Gamma Analysis

In this study, all plans were measured with a pre-calibrated MatriXX in its functionally designed solid water phantom. We kept the fluence and leaf sequencings unchanged and reset the angles of the gantry and the collimator zero. To decrease the potential masking error for the perpendicular composite (PC) method indicated by the AAPM TG-218 reports,<sup>13</sup> we calculated the gamma passing rate for each beam, respectively. Let  $\{r_r\}$  be the set of reference points in the simulated plane,  $\{r_e\}$  be the set of evaluated points in the measurement plane, the gamma index at  $r_r$  is computed by

$$\Gamma(r_e, r_r) = \sqrt{\frac{|r_e - r_r|^2}{\Delta d^2} + \frac{|D_e(r_e) - D_r(r_r)|^2}{\Delta D_A^2}} \quad (1)$$

$$\Delta D_A = \Delta D \cdot D_{\max, \{r_e | D_e(r_e) \geq cD_{\max}\}}$$

$$\gamma(r_r) = \min\{\Gamma(r_e, r_r)\} \forall \{r_e\}$$

with  $|r_e - r_r|$  indicating the spatial distance and dose differences,  $\Delta d$  the DTA criterion,  $D_{\max}$  the maximum value of the measured dose,  $\Delta D$  the dose difference

criterion, and  $c$  the cut-off threshold. Conventionally,  $\{r_e\}$  is defined by the computational domain of gamma analysis, where the points with a measured dose higher than  $cD_{\max}$  could be considered. The dose discrepancy at  $r_r$  is acceptable, if  $\gamma(r_r) \leq 1$ . In this study, multiple combinations of  $\Delta D/\Delta d$  (from 2%/2 mm to 5%/5 mm) and  $c$  (from 5% to 20%) were considered to evaluate the performance of the conventional planar gamma analysis.

### Modified Scheme

As illustrated in Figure 1A, we designated the beam projections over their iso-centric (ISO) planes as the computational domain for gamma analysis. The similarity transformation in Figure 1B was applied to calculate the projection. Similarly, to avoid the masking errors due to the summation, we suggested to project the beams one after another and compute the corresponding gamma passing rate, respectively. Figure 1C illustrates the modified computational domain with the planned and measured dose overlaying. Besides, to present the ROI-specific QA results, we also designated the projections of PTV and OAR as the computational domain for gamma analysis. We computed the ROI projections from each beam eye view and performed the gamma analysis to avoid the masking error. The  $D_{\max}$  in Eq. (1) was also substituted by  $D_r(r_r)$  to make the local analysis more accurate.

Furthermore, since it was commonly interested to inspect the adequate dose coverage of PTV, we assessed its dose discrepancy by calculating the ratio of points failing the gamma test with a measured dose lower than the planned one (hereafter referred to as cold spots). On the other hand, it was commonly interested to inspect the adequate dose sparing of OAR. Therefore, the ratio of failed points with a measured dose higher than the planned one (hereafter referred to as hot spots) contributed to evaluating the dose discrepancy of OAR. Furthermore, to distinguish for the cold-spot ratio of PTV or hot-spot ratio of OAR, a minus or positive sign was added for the gamma index in Eq. (1).

Figure 1D demonstrated the ROI-specific gamma analysis with PTV and spinal cord concerned, where the contours of PTV, spinal cord, and beams projections were in red lines, white lines, and black lines, respectively. We overlapped the projections from different BEVs. Therefore, there were several white lines. Figure 1E demonstrated the overall diagram of the proposed method. The planned dose, measured dose, and treatment plans were exported in DICOM format to the Matlab R2015a (The Math Works, MA, USA) for data processing.

### Model Validation

To evaluate the performance of the proposed method, we randomly selected 6 IMRT patients' data from the database of Sichuan Cancer Hospital, with the detailed information described in Table 1. The treatments were planned with the Eclipse TPS (version 11.0.42, Varian Medical Systems, Palo Alto, CA) and were delivered by the Varian 23EX linear accelerator with nominal 6 Mv photon beams.

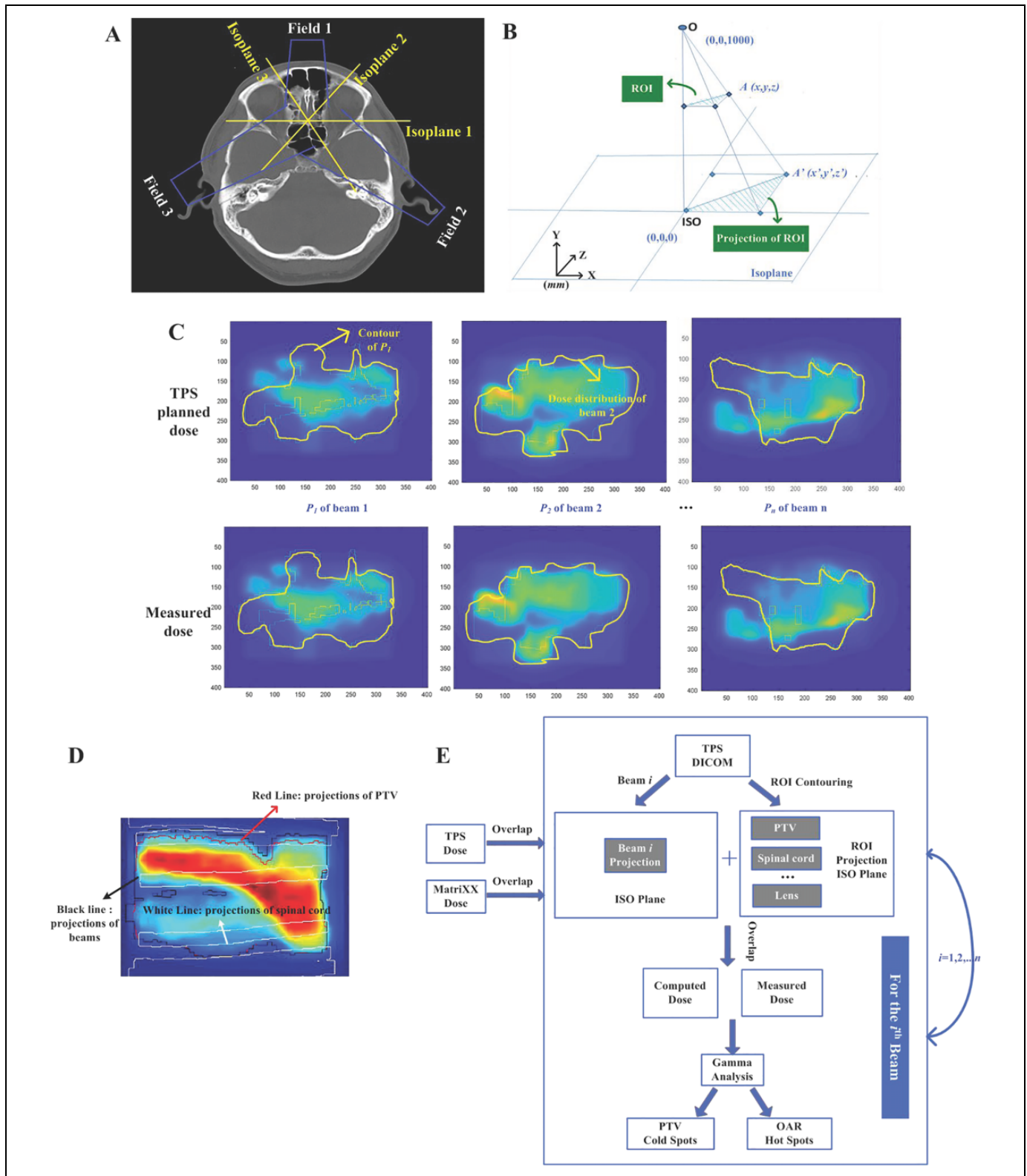


**Figure 1.** Illustration of the beam-projection based gamma analysis. (A) 2D sketch of the beams and their coherent iso-planes. (B) 3D sketch of ROI projection from the beam eye view (BEV), calculated by similarity transformation. The ISO point is at the origin of the axis.  $O$  is the source point. The source axis distance is of 1 m. (C) Computational domain of the proposed method. The contour of the  $i$ th beam projection is in yellow lines and overlaps with its coherent dose distribution. (D) ROI specific computational domain. Overlapped with the dose distribution, the projective contours of PTV and spinal cord are in red and white lines, respectively. The projective contours of beams are in black line. (E) Flow diagram of the proposed method.

**Table 1.** Clinical Parameters of the Tested Cases.

Case Num.	Disease	PTV Vol (ccm)	Beam Num.	Key OAR	Dose Pre. (Gy/f)
1	Cer cancer	1229.7	7	SP, Bl, In, Kid, Liver, Pan.	45/25
2	Lung cancer	633.1	7	Heart, Lung, SP, Tr	60/30
3	Lung cancer	435.1	7	Heart, Lung, SP, Tr	60/30
4	Lung cancer	401.2	6	Heart, Lung, SP, Tr	50/20
5	Lung cancer	612.9	7	Heart, Lung, SP, Tr	60/30
6	NPC	219.2	7	Lens, BS, BS, Parotid	66/30

Abbreviations: Num, number; Eso, esophagus; NPC, nasopharyngeal carcinoma; Vol, volume; ccm, cubic centimeter, PTV, planning target volume; OAR, organ at risk; Cer, cervical; SP, spinal cord; Bl, bladder; In, intestine; Kid, kidney; Pan, pancreas; Tr, trachea; BS, brain stem; Gy/f, Gy per fraction.

We assessed the performance of the proposed method by computing the gamma passing rates with the conventional and modified gamma analysis schemes. To evaluate the difference in gamma passing rates, we conducted a two-sided Wilcoxon signed-rank test in the Matlab R2015a software, with a  $P$  value  $<0.05$  regarded as significant. The ROI-specific gamma analysis was also conducted. Furthermore, a 7.09% dose error was specially introduced to evaluate the performance. Figure 2 illustrated the dose error, which was near the right retina of the sixth patient. It was created by manually changing the multileaf collimator (MLC) position of the fourth beam in the Eclipse TPS. The dose distributions of the error-free (EF) and error-included (EI) plans were also demonstrated.

## Results

Table 2 compares the gamma passing rates of the 6 tested cases between the conventional gamma analysis method and the proposed method. To avoid the masking errors accumulated during the summation,<sup>13</sup> we computed the gamma passing rates beam after beam and averaged the values in both methods. The gamma criterion ranged from 2%/2 mm to 5%/5 mm in both methods. The computational domain of the proposed method was the beam projections, while it varied along with the cut-off thresholds in the conventional method. Therefore, a significant difference was observed among the conventional gamma passing rates. In comparison, the gamma passing rates in the proposed method were all higher than 90%. The result of the gamma passing rate in the modified method was conformable to that in the conventional method with a cut-off threshold of 5%. Besides, the modified scheme also had a lower value of variation than that of the conventional scheme.

Table 3 demonstrated the results of the ROI-specific gamma analysis achieved by the modified scheme. Again, to avoid the masking error, the gamma passing rate was computed in terms of each beam and averaged finally. The gamma passing rate for the PTV was computed. Besides, considering the location of the tumor, we selected the spinal cord to be the concerned OAR for cases 1 to 5, while the brain stem and lens for the sixth case. It was noted the gamma passing rate for the PTV was very close to that of the beam projection in Table 2. The gamma passing rate for the OAR decreased considerably in some cases. The proposed method could generate ROI-specific results in terms of the gamma passing rate.

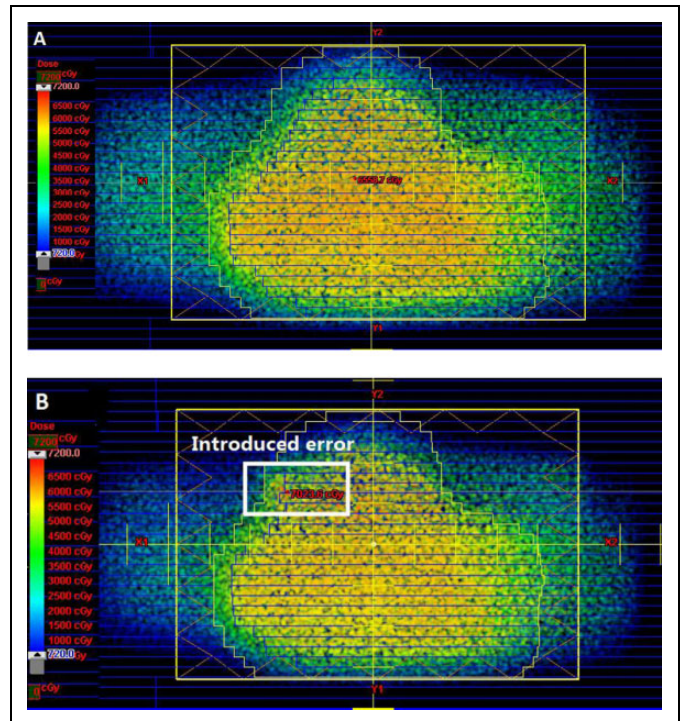


**Figure 2.** Illustration for the dose error. The dose distribution of the fourth beam in the sixth patient was demonstrated in (A). By editing the MLC, a 7.1% dose error was introduced, and the resultant dose distribution was shown in (B). (A) Dose distribution of the error-free (EF) plan, the maximum dose was 65.59 Gy. (B) Dose distribution of the error-included (EI) plan, the maximum dose was 70.24 Gy.

Figure 3 shows the cold spots ratio of PTV and hot spots ratio of OAR with various gamma criteria. The resultant ratio increased under the more rigorous criterion.

Figure 4 displayed the gamma passing rates for the error-free (EF) and error-included (EI) plans, where the results of the conventional (Con) and the modified (Mo) schemes were both evaluated under various gamma criteria. The resultant discrimination of error was less than 2% in the conventional scheme, while it was improved to 5% by the modified one.

## Discussion

In this study, we implemented a modified gamma analysis scheme to improve the clinical significance of the planar QA

**Table 2.** Comparison of Gamma Passing Rates.

$\Delta D/\Delta d$	2mm/2%	3mm/3%	4mm/4%	5mm/5%
Conventional method				
Cut-off threshold				
5%	90.15 ± 3.34	92.08 ± 3.15	94.29 ± 2.42	96.23 ± 2.06
10%	88.72 ± 5.36	91.13 ± 3.72	92.26 ± 3.68	94.51 ± 3.14
20%	86.49 ± 6.20	90.03 ± 4.83	91.53 ± 4.06	92.27 ± 4.49
Proposed method	90.79 ± 3.25	93.65 ± 1.89	96.27 ± 1.04	99.04 ± 0.87

The gamma passing rate are listed as (mean ± standard deviation).

**Table 3.** Results of the ROI-Specific Gamma Analysis by the Proposed Method.

ROI	PTV	Spinal cord	Brain stem	Lens
$\Delta D/\Delta d$				
5mm/5%	99.30 ± 0.51%	97.14 ± 2.65%	95.43 ± 1.75%	96.45 ± 2.49%
4mm/4%	96.82 ± 2.05%	93.04 ± 5.27%	85.17 ± 4.09%	91.37 ± 3.01%
3mm/3%	94.31 ± 1.98%	89.17 ± 11.95%	77.65 ± 9.94%	80.96 ± 11.30%
2mm/2%	91.54 ± 2.59%	68.32 ± 16.84%	66.28 ± 15.35%	65.03 ± 18.65%

The gamma passing rate are listed as (mean ± standard deviation).

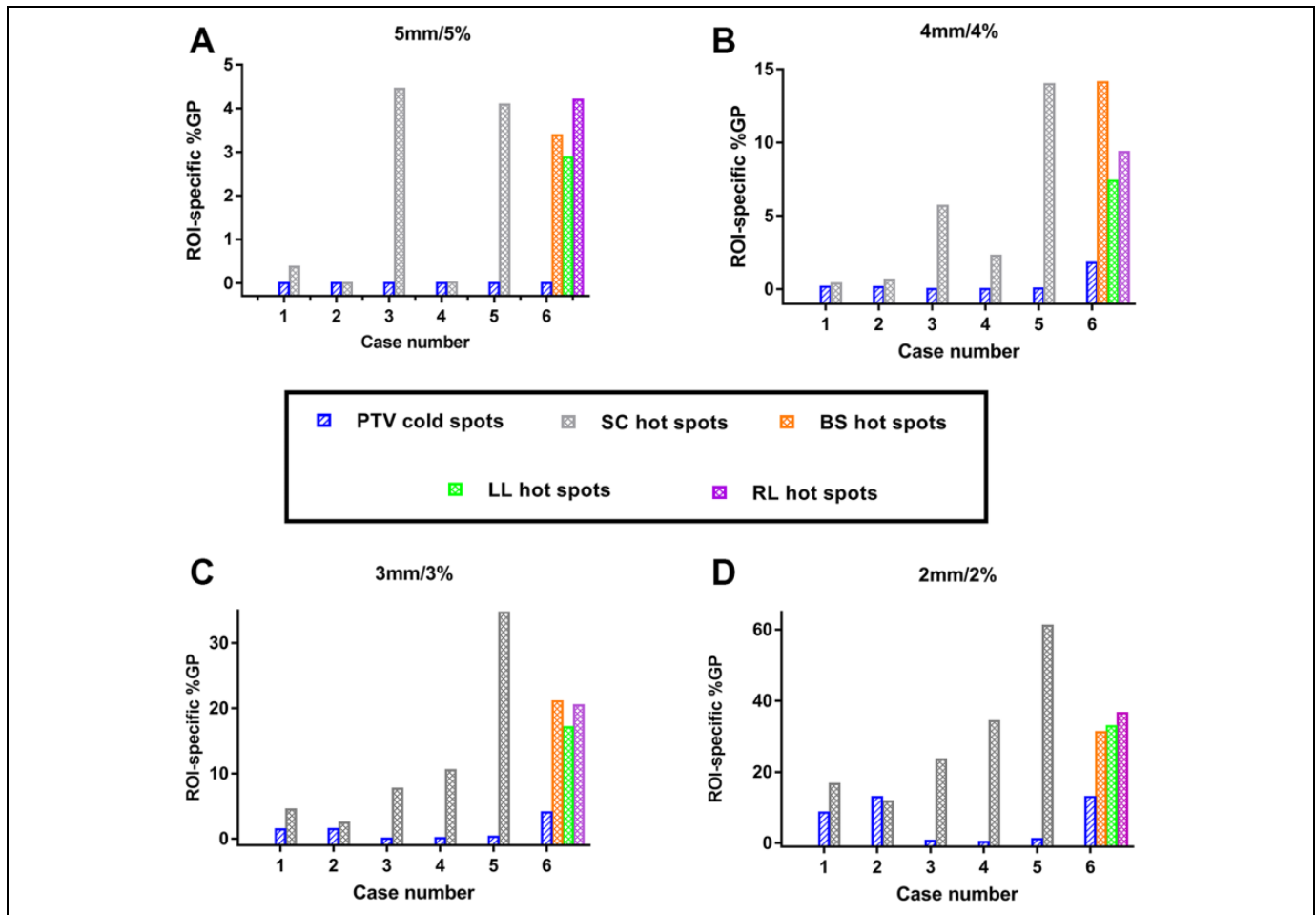


**Figure 3.** Cold and hot spots ratio with various  $\Delta D/\Delta d$ . The cold spots ratio of PTV, and the hot spots ratio of spinal cord (SP), brain stem (BS), left lens (LL), right lens (RL) were computed. (A)  $\Delta D/\Delta d$  was 5mm/5%. (B)  $\Delta D/\Delta d$  was 4mm/4%. (C)  $\Delta D/\Delta d$  was 3mm/3%. (D)  $\Delta D/\Delta d$  was 2mm/2%.



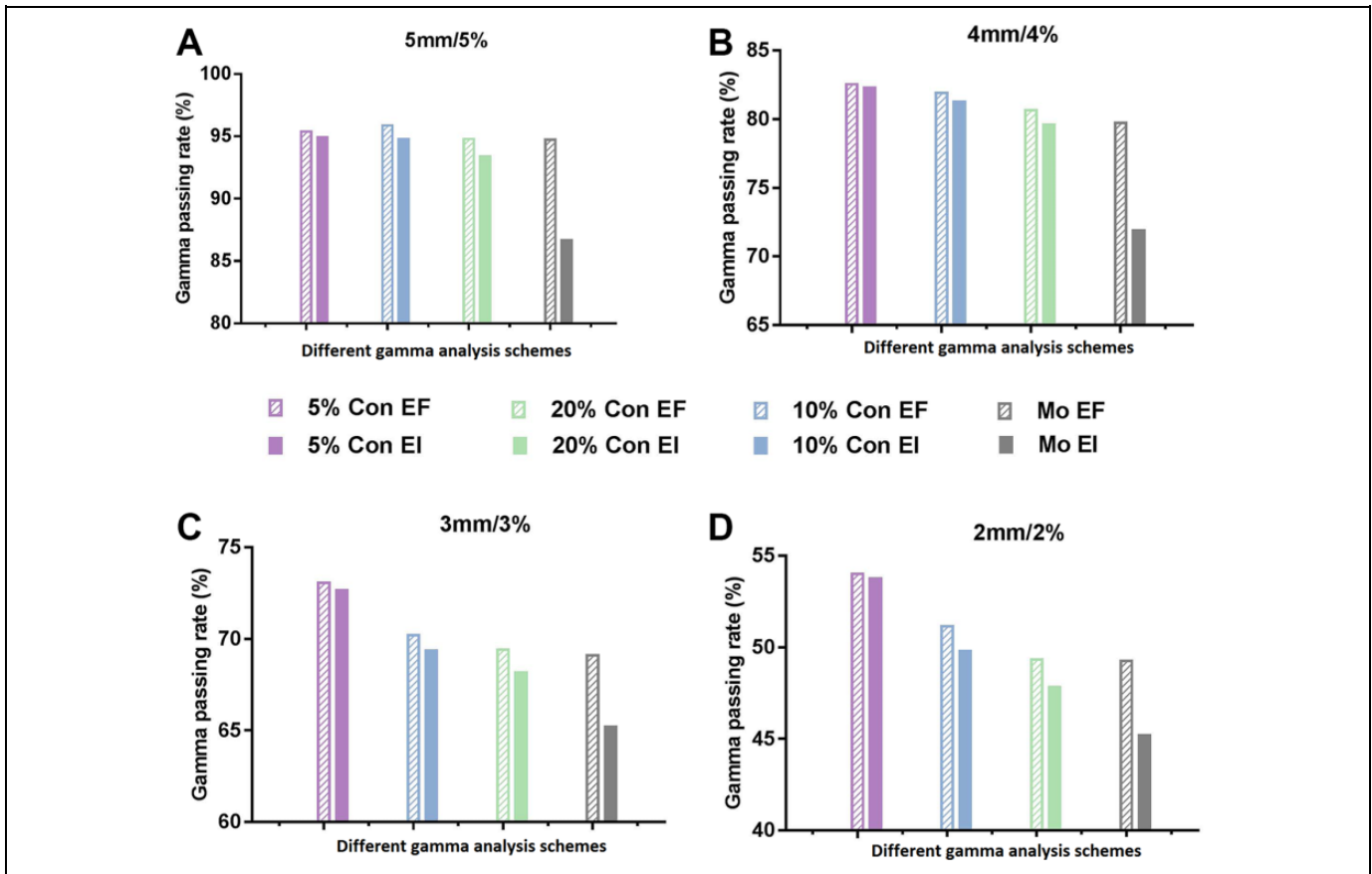


**Figure 4.** Comparison of gamma passing rates with and without introduced dose error. The results were computed by the conventional (Con) and the modified methods (Mo). EF denoted for the error-free plan, while EI denoted for the error-included plan. (A)  $\Delta D/\Delta d$  was 5mm/5%. (B)  $\Delta D/\Delta d$  was 4mm/4%. (C)  $\Delta D/\Delta d$  was 3mm/3%. (D)  $\Delta D/\Delta d$  was 2mm/2%.

results. The key novelty was to take the projections of beam and ROI to be the computational domain of the gamma analysis, thereby potentially correlating the dose discrepancy with clinical treatment.

According to the TG 218 report,<sup>13</sup> a more accurate result should be expected from the ROI-specific gamma analysis. However, the conventional scheme could hardly achieve. Comparatively, the modified scheme was able to identify the ROI-specific dose discrepancy, as validated by Table 3 and Figure 3. Therefore, individualized QA results could be provided. For instance, we could set the acceptable threshold of each OAR separately in terms of its planned dose. The acceptance threshold of the spinal cord should be more rigorous when the planned dose is close to 45 Gy.

The modified scheme could also give us some insight into the individualized treatment. For example, the hot spot ratio of the sixth case was significantly higher than that in other cases. The reason could be the challenging treatment plan of the head-and-neck tumor, where the therapeutic window for radiation could be very narrow to mimic the irregular shape of lesions and avoid the proximity of multiple OAR. To identify the cause, a subsequent re-inspection and error tracing process could be implemented.

The proposed method might also help to distinguish the existing error for the concerned ROI, according to the result in Figure 4. Since we have reduced the computational region along with the ROI, the error ratio could be lifted compared with that in the conventional method where additional region outside the ROI is concerned. Accordingly, the systematical evaluation of the error sensitivity is a topic of our future works, where the number of testing cases should be expanded, and the 3D dose verification should be implemented.

While this study could provide a more clinically explicable system to evaluate the dose verification result, it is still important to discuss its limitations. First, since the dose output of each control point is not able to be obtained in our current TPS system, the present scheme did not apply to the VMAT treatments. However, the proposed method is a general methodology. Therefore, it should be suitable for various treatment techniques with the VMAT included. Second, the proposed method could only partially maintain the individualized spatial information during the dose verification process, and the full 3D geometry information has not been reserved. On the one hand, we are unable to identify the actual anatomy position for dose discrepancy. The 3D dose verification methods,<sup>11,12</sup> could address this problem. However, it could lead to problems for

error accumulation during the 2D-3D transformation process and exacerbated computational efficiency. On the other hand, the proposed method is a compromise between the computational cost and the clinical significance. It could be implemented efficiently with the widely used planar gamma analysis system, without the requirement for additional investment. Finally, it is still tough to identify the precise cause of the dose discrepancy due to the error-cumulative nature of dose distribution, where the imperfection of the gantry, collimator, and motions of leaves could involve. Therefore, new devices<sup>14</sup> and techniques<sup>8</sup> could be expected for further investigation.

## Conclusion

In this study, we have established and investigated an in-house modified gamma analysis system to assess the QA result in terms of clinical significance. Compared with the conventional scheme, the modified one could provide both the dose inspection result and the ROI-specific discrepancy result. It could be conveniently integrated into the conventional dose verification process, particularly for less developed regions where high-end 3D dose verification devices are not affordable.

## Authors' Note

Author for statistical analysis: Yiling Wang (mara.wangyiling@gmail.com).


## Declaration of Conflicting Interests

The author(s) declared no potential conflicts of interest with respect to the research, authorship, and/or publication of this article.

## Funding

The author(s) disclosed receipt of the following financial support for the research, authorship, and/or publication of this article: This work was supported by the National Natural Science Foundation of China (NSFC) under Project No. 61901087, China Postdoctoral Science Foundation under Project No. 2019M663471, Chengdu Science and Technology Bureau under Project No. 2019YF0500022SN, Sichuan Science and Technology Program under Project No. 2019YJ0581, No. 2019YJ0584, No. 2019YFG0185, and Science and Technology bureau of LiangShan, Sichuan Province under Project No. 18YYJS0105.

## ORCID iD

Yiling Wang  <https://orcid.org/0000-0003-3619-4532>

## References

- Nelms BE, Zhen H, Tomé WA. Per-beam, planar IMRT QA passing rates do not predict clinically relevant patient dose errors. *Med Phys*. 2011;38(2):1037-1044.
- Zhen H, Nelms BE, Tome WA. Moving from gamma passing rates to patient DVH-based QA metrics in pretreatment dose QA. *Med Phys*. 2011;38(10):54775489.
- Ezzell GA, Burmeister JW, Dogan N, et al. IMRT commissioning: multiple institution planning and dosimetry comparisons, a report from AAPM Task Group 119. *Med Phys*. 2009;36(11):5359-5373.
- Low DA, Harms WB, Mutic S, Purdy JA. A technique for the quantitative evaluation of dose distributions. *Med Phys*. 1998;25(5):656-661.
- Dobler B, Streck N, Klein E, Loeschel R, Haertl P, Koelbl O. Hybrid plan verification for intensity-modulated radiation therapy (IMRT) using the 2D ionization chamber array IMRT MatriXX—a feasibility study. *Phys Med Biol*. 2010;55(2):N39-N55.
- Fakir H, Gaede S, Mulligan M, Chen JZ. Development of a novel ArcCHECK<sup>TM</sup> insert for routine quality assurance of VMAT delivery including dose calculation with inhomogeneities. *Med Phys*. 2012;39(7):4203-4208.
- Chandraraj V, Stathakis S, Manickam R, Esquivel C, Supre SS, Papanikolaou N. Comparison of four commercial devices for RapidArc and sliding window IMRT QA. *J Appl Clin Med Phys*. 2011;12(2):3367.
- Wootton LS, Nyflot MJ, Chaovalitwongse WA, Ford E. Error detection in intensity-modulated radiation therapy quality assurance using radiomic analysis of gamma distributions. *Int J Radiat Oncol Biol Phys*. 2018;102(1):219-228.
- Stasi M, Bresciani S, Miranti A, Maggio A, Sapino V, Gabriele P. Pretreatment patient-specific IMRT quality assurance: a correlation study between gamma index and patient clinical dose volume histogram. *Med Phys*. 2012;39(12):7626-7634.
- Oldham M, Thomas A, O'Daniel J, et al. A quality assurance method that utilizes 3D dosimetry and facilitates clinical interpretation. *Int J Radiat Oncol Biol Phys*. 2012;84(2):540-546.
- Sdrolia A, Brownsword KM, Marsden JE, Alty KT, Moore CS, Beavis AW. Retrospective review of locally set tolerances for VMAT prostate patient specific QA using the COMPASS((R)) system. *Phys Med*. 2015;31(7):792-797.
- Kadoya N, Saito M, Ogasawara M, et al. Evaluation of patient DVH-based QA metrics for prostate VMAT: correlation between accuracy of estimated 3D patient dose and magnitude of MLC misalignment. *J Appl Clin Med Phys*. 2015;16(3):5251.
- Miften M, Olch A, Mihailidis D, et al. Tolerance limits and methodologies for IMRT measurement-based verification QA: Recommendations of AAPM Task Group No. 218. *Med Phys*. 2018;45(4):e53-e83. doi:10.1002/mp.12810
- Carlone M, Cruje C, Rangel A, McCabe R, Nielsen M, Macpherson M. ROC analysis in patient specific quality assurance. *Med Phys*. 2013;40(4):042103.